LA-UR-19-27122
Approved for public release; distribution is unlimited.

Title: Direct Disposal of Dual Purpose Canisters – LANL – Boral Solubility (FY19)

Author(s): Caporuscio, Florie Andre
Sauer, Kirsten Benedict
Rock, Marlena Joyce

Intended for: Report

Issued: 2019-07-23

Direct Disposal of Dual Purpose Canisters – LANL – Boral Solubility (FY19)

Fuel Cycle Technology

Prepared for
U.S. Department of Energy
Spent Fuel & Waste Science and Tech
Caporuscio, F.A.
Sauer, K.B.
Rock, M. J.
Los Alamos National Laboratory

July 30, 2019
SF-19LA01030503
LA-UR-19-#####

SUMMARY

Three baseline hydrothermal experiments were conducted with deionized water and Neutron Absorber Composite, a commercially product manufactured by 3M^{TM} (referred to by its former title, Boral®, in this report). Boral® is composed of boron carbide (B_4C) sintered with Al and encased with aluminum cladding. Hydrothermal experiments were conducted 150, 230, and 300 °C and 150 bar for two weeks. Changes in the physical properties and mineralogy of the Boral® coupons were characterized with X-ray diffraction and scanning electron microscopy. Compositions of reaction fluids were monitored during and after each experiment. Results indicate that alteration of aluminum cladding to boehmite (AlO(OH)) occurs over the range of investigated temperatures but is most significant at 300 °C. The formation of boehmite is accompanied with H_2 gas. The crystal structure of boron carbide (B_4C) appears to be unaltered by hydrothermal treatment; however aqueous boron was present in the reaction fluids.

CONTENTS

FIGURES

TABLES

ACRONYMS

BWR – Boiling Water Reactor

DPC – Dual Purpose Canister

EDX – Energy Dispersive X-ray

EPA – Environmental Protection Agency

FY – Fiscal Year

IAEA – International Atomic Energy Association

IC - Ion Chromatography

PWR – Pressurized Water Reactor

SEM - Scanning Electron Microscope

SFWST - Spent Fuel and Waste Science and Technology R&D

XRD - X-ray Diffraction

DIRECT DISPOSAL OF DUAL PURPOSE CANISTERS – LANL – BORAL SOLUBILITY

1. INTRODUCTION

The United States Department of Energy's Spent Fuel and Waste Deposition program aims to investigate the design and safety function of generic geologic repositories. Currently, most spent fuel and waste are kept in dry storage at the site of production in dual-purpose canisters (DPCs), which are intended for storage and transportation. The U.S. is investigating the possibility of disposing waste permanently within DPCs based on multiple factors, including the reduction of waste, worker dose, and cost. The largest existing DPCs hold up to 37 pressurized water reactor (PWR) or 89 boiling water reactors (BWR) assemblies (Greene et al., 2003). As a result, DPCs are associated with higher thermal loads than considered by foreign countries (IAEA, 2000) and the need for criticality control materials (neutron absorber composites, SAND, 2017). In the case of canister breach within a repository setting, it is important to understand the material properties of neutron absorber composites with groundwater and other engineered barrier materials in order to assess the long-term safety and function of a repository.

This report presents a baseline study on the hydrothermal reactivity of deionized water with Neutron Absorber Composite, a commercially product manufactured by 3M^{TM} (referred to by its former title, Boral®, in this report). Boral® is composed of boron carbide (B_4C) sintered with Al and encased with aluminum cladding. Hydrothermal experiments were conducted 150, 230, and 300 °C and 150 bar for two weeks. Changes in the physical properties and mineralogy of the Boral® coupons were characterized with X-ray diffraction and scanning electron microscopy. Compositions of reaction fluids were monitored during and after each experiment. Results indicate that alteration of aluminum cladding to boehmite (AlO(OH)) occurs over the range of investigated temperatures but is most significant at 300 °C. The formation of boehmite is accompanied with H_2 gas. The crystal structure of boron carbide (B_4C) appears to be unaltered by hydrothermal treatment; however aqueous boron was present in the reaction fluids.

1.1 Background and Objective

In the United States, the use of DPCs for storage and subsequent disposal has been proposed (Greenburg and Wen, 2013). The design the canister varies, but will likely be constructed from steel or stainless steel with a steel reinforced concrete overpack and a neutron

absorber composite material (IAEA, 2000). The proposed dual-purpose canisters for US repositories may contain up to 37 spent fuel assemblies (e.g., PWR), while many of the European concepts are limited to four spent fuel assemblies (4-PWR) (Pusch, 2008; Greenburg and Wen, 2013). This increased number of spent fuel assemblies within the US dual-purpose canisters will generate a greater amount of heat within the waste package. For example, high-level modeling suggests a 32-PWR waste package (at 60 gigawatt-days per metric ton burnup) disposed in a clay/shale host rock, has the potential to reach 299 °C after 85 years at the canister surface (25 years ventilation; 15 m package spacing; Greenberg and Wen, 2013). This is just one of many models/designs for canister configurations in a U.S. nuclear repository, but provides an example of a high temperature scenario (Figure 1). Further, the thermal evolution of this potential repository design demonstrates the need for high temperature experimental work on the interaction in canister materials and water that have not been explored previously by the European programs. The following summarizes previous research relevant to the stability of Boral® under hydrothermal conditions.

Early research on aluminum corrosion by Hunter and Fowle (1956) describe oxide film formation on aluminum, the thickness of which is a function of temperature. The oxide phases were not determined. A comprehensive review by Diggle et.al. (1968) on anodic oxide films produced on aluminum surfaces described that the most prevalent surface coating was boehmite. Weeks (1978) considered corrosion of Boral® in spent fuel storage pool racks. He investigated conditions of pH 5.0 to 8.5 and temperatures between 100 to 175 °C. Significantly, Weeks identified swelling of the Boral® components due to aluminum corrosion. The corrosion reaction produced Al_2O_3 , however the authors did not describe how this was characterized, and H_2 gas within 5 days of reaction. The swelling phenomena was not well characterized for mineral reactions. Weeks did not expect B_4C loss by corrosion of Boral®.

Walters (1985) provided an electrochemical study of Boral® corrosion. Performed at 23 °C over a period of a few days, the experiment using distilled water generated 0.045 millimoles of H_2 gas. Walters (1985) predict that the BORAL® would delaminate in as soon as 11 years in his experimental conditions. Differences in temperature, pressure and time prevent direct comparison with our experiments.

The dissertation of Wierschke (2015) on the evaluation of neutron absorbing compounds for interim storage of used nuclear fuel focuses of aluminum oxidation in both dry and wet

environments over a range of temperatures. Dry oxidation research spanned temperatures from 70 to 700 °C. Experiments on the effect of humidity on neutron absorber corrosion at temperatures between 300 and 570 °C were also conducted. The 300 °C experiment (217 days) performed indicate no consistent change in dimensions but a mass loss. Wierschke (2015) attributes the mass loss to boron leaching.

Konings et al. (2012) describe aluminum hydroxide mineral stability under humid conditions and intermediate temperatures. Metastable phases such as bayerite (200 to 300 °C) and boehmite (300 to 500 °C), are present. In a wet oxidation scenario at temperatures up to 570 °C, bayerite (≤ 77°C) will grow and transition to pseudoboehmite (up to 100 °C). Above 100 °C, crystalline boehmite is stable. For both bayerite and pseudoboehmite, gelatinous boehmite is the precursor to both crystalline phases in the wet environment.

Santos, et al. (2009) describe methods to synthesize boehmite at 200 °C in a variety of crystal morphologies, including: ellipsoidal, rhombic, hexagonal, and lath-like, depending on the precursor materials.

The SAND (2017) report is a review document intended to produce a work plan on how to demonstrate filler emplacement in small-scale representations of DPCs. It is useful in understanding design components and materials used for DPCs. Furthermore, it identified parameters such as fuel cladding temperature limits (350 °C), thermal histories, criticality assumptions, incident scenarios, pressure containment designs, etc. The report notes that the aluminum plus water reaction within a single DPC would create Al_2O_3 and generate 30 kmoles of H_2 gas.

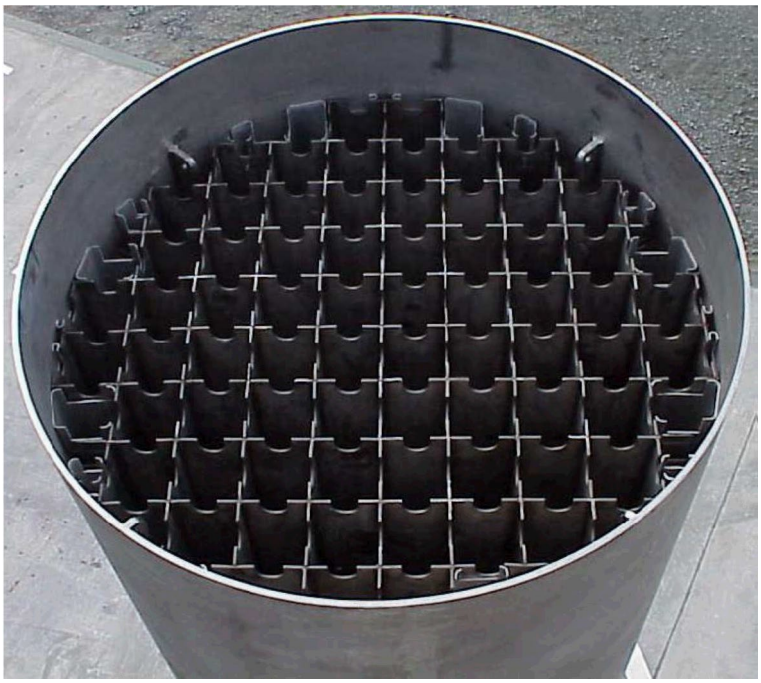

Figure 1: View of MPC-68 shell and basket (from Greene et al. 2013).

2. METHODS and MATERIALS

2.1 Materials

Boral® is composed of a core of ceramic-metal composite material composed of boron carbide and aluminum and clad in aluminum metal. The composite core is produced by sintering boron carbide powder with atomized aluminum powder and has a porosity of ~5% (EPRI, 2009). The boron carbide grains are between 75 and 250 μm (EPRI, 2009). The Boral® used in this study was sourced from 3M Advanced Materials Division, Ceradyne, a 3M company. It has a thickness of 0.3 cm and was cut into rectangular coupons with the approximate dimensions of 1.3 cm x 3.8 cm.

2.2 Experimental Setup

Initial components for each experiment are summarized in Table 1. Experiments included either two or three coupons of Boral® with the approximate dimensions: 3.8 cm length, 1.3 cm width, and 0.3 cm height. The remaining volume of the reaction cell was filled with deionized water.

Experiments were conducted in a flexible gold reaction cell and fixed into a 500 mL Gasket Confined Closure reactor (Seyfried et al., 1987). Experiments were pressurized to 150 to

160 bar and were heated isothermally to 300, 230, or 150 °C for two weeks. Reaction fluids were extracted during the experiments and analyzed to investigate the aqueous geochemical evolution in relationship to mineralogical alterations. The sampled reaction liquids were split three-ways producing aliquots for unfiltered anion, unfiltered cation, and filtered (0.45 μm syringe filter) cation determination. All aliquots were stored in a refrigerator at 1 °C until analysis.

Table 1: Run conditions. Number in parentheses indicates number of coupons included in the experiment.

Exp.	Components	Run Temp. (°C)	Pressure (bar)	Run time
BRL-1	Boral® (3) + DI	300	150	2 weeks
BRL-2	Boral® (2) + DI	150	150	2 weeks
BRL-3	Boral® (3) + DI	230	150	2 weeks

2.3 Characterization Methods

The dimensions and masses of the Boral® coupons were measured before experiments BRL-2 and BRL-3. The Al surface and the B_4C-Al core of a Boral® coupon was scanned with X-ray diffraction (XRD) to characterize mineralogy the starting materials. The core of a Boral® coupon was exposed by filing and also characterized with XRD. These same methods were repeated on post reaction coupons.

Analytical electron microscopy was performed using a FEITM Inspect F scanning electron microscope (SEM). All samples were Au/Pd-coated prior to SEM analysis. Imaging with the SEM was performed using a 5.0 kV accelerating voltage and 1.5 spot size. Energy dispersive X-ray spectroscopy (EDX) was performed at 30 kV and a 3.0 spot size.

Major cations and trace metals in aqueous fluids were analyzed via inductively coupled plasma-optical emission spectrometry (Perkin Elmer Optima 2100 DV) and inductively coupled plasma-mass spectrometry (Elan 6100) utilizing EPA methods 200.7 and 200.8. Ultra-high purity nitric acid was used in sample and calibration preparation prior to sample analysis. Internal standards (Sc, Ge, Bi, and In) were added to samples and standards to correct for matrix effects. Standard Reference Material (SRM) 1643e Trace Elements in Water was used to check the accuracy of the multi-element calibrations. Inorganic anion samples were analyzed by ion chromatography (IC) following EPA method 300 on a Dionex DX-600 system. Aqueous geochemical results are presented in Appendix A.

3. RESULTS

3.1 Physical Changes

The Boral® coupons included in the experiments experienced physical changes (Figure 2, Table 2). The length, width, and height and mass of the rectangular pieces increased, with the most dramatic effects observed in the 300 °C experiment (BRL-1, Figure 2a). The expansion of the coupons corresponded with a density decrease. Table X records the dimension and mass changes, as well as calculated volumes and densities. The following describes the physical changes observed in the three experiments.

BRL-1, 300°C: Coupons reacted at 300 °C expanded in all directions, resulting in an average volume increase of 90±3%. Coupons are slightly thicker at the edges with a depression in the center. The color of the aluminum cladding changed from shiny metal to matte grey or white powder (Figure 2a). The mass of each of the three coupons increased by ~2.1 g, corresponding to a 54% gain.

BRL-2, 150°C: Coupons reacted at 150 °C experienced very little change in dimensions (Table 2), corresponding to ~1% volume increase, which may reflect uncertainty in measurement. The coupon thickness did not increase. The coupons appear unwarped; the major physical difference is a thin coating of white powdery mineralization on the Al cladding (Figure 2b). The mass of each coupon increased by ~0.06 g, corresponding to ~1% mass increase.

BRL-3, 230°C: Coupons reacted at 230 °C show slight dimension increases, corresponding to a 4% volume gain. The thickness (height) of the coupon did not increase, similarly to BRL-2. The surface of the coupons are coated in a powdery, white mineral (Figure 2c). The mass of each coupon increased by 0.14 to 0.15 g, corresponding to an average gain of 3.7%.

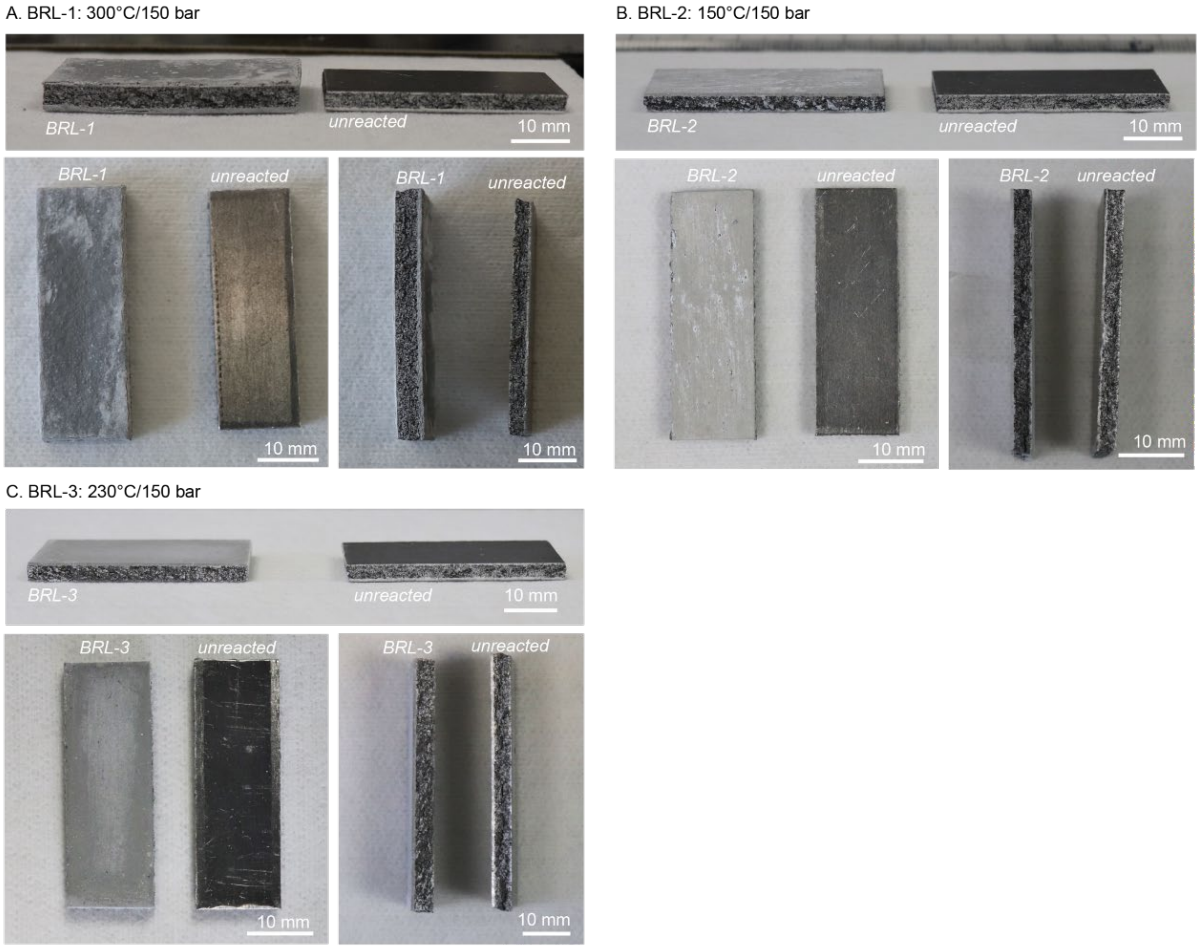

Figure 2: Photos of reacted coupons from each Boral® experiment, **[A]** BRL-1, **[B]** BRL-2, and **[C]** BRL-3, next to a representative unreacted coupon.

Table 2: Boral® coupon dimensions, masses, and calculated volumes and densities

SAMPLE	Length (cm)	Width (cm)	Height (cm)	Volume (cm^3)	Volume differential (cm^3)	Volume change (%)	Mass (g)	Mass differential (g)	Mass change (%)	Density (g/cm^3)
BRL-1										
Pre-experiment										
BRL-1 Average coupon	3.80	1.30	0.32	1.58	–	–	3.889	–	–	**2.46**
BRL-1 Post-experiment										
BRL-1-coupon1	4.11	1.46	0.51	3.06	1.48	93.6	6.121	2.232	57.4	2.00
BRL-1-coupon2	4.07	1.42	0.51	2.95	1.37	86.5	5.909	2.020	51.9	2.00
BRL-1-coupon3	3.98	1.47	0.51	2.98	1.40	88.8	5.991	2.102	54.1	2.01
Average					**1.42**	**89.6**		**2.118**	**54.5**	**2.00**
Standard Deviation					**0.05**	**3.0**		**0.087**	**2.2**	**0.00**
BRL-2										
Pre-experiment										
BRL-2-long	3.80	1.31	0.32	1.59	–	–	4.011	–	–	2.52
BRL-2-short	3.72	1.32	0.32	1.57	–	–	3.896	–	–	2.48
Post-experiment										
BRL-2-long-reacted	3.90	1.31	0.32	1.63	0.04	2.6	4.073	0.063	1.6	2.49
BRL-2-short-reacted	3.72	1.33	0.32	1.58	0.01	0.8	3.954	0.058	1.5	2.50
Average					**0.03**	**1.7**		**0.060**	**1.5**	**2.49**
Standard Deviation					**0.02**	**0.9**		**0.003**	**0.0**	**0.00**
BRL-3										
Pre-experiment										
BRL-3-coupon1	3.84	1.31	0.32	1.61	–	–	3.957	–	–	2.46
BRL-3-coupon2	3.74	1.30	0.32	1.56	–	–	3.835	–	–	2.46
BRL-3-coupon3	3.86	1.32	0.32	1.63	–	–	4.015	–	–	2.46
Post-experiment										
BRL-3-coupon1	3.88	1.34	0.33	1.72	0.11	6.6	4.110	0.152	3.9	2.40
BRL-3-coupon2	3.77	1.32	0.32	1.59	0.04	2.4	3.974	0.139	3.6	2.50
BRL-3-coupon3	3.89	1.32	0.33	1.69	0.06	3.9	4.166	0.151	3.8	2.46
Average					**0.07**	**4.3**		**0.147**	**3.7**	**2.45**
Standard Deviation					**0.03**	**1.7**		**0.006**	**0.1**	**0.04**

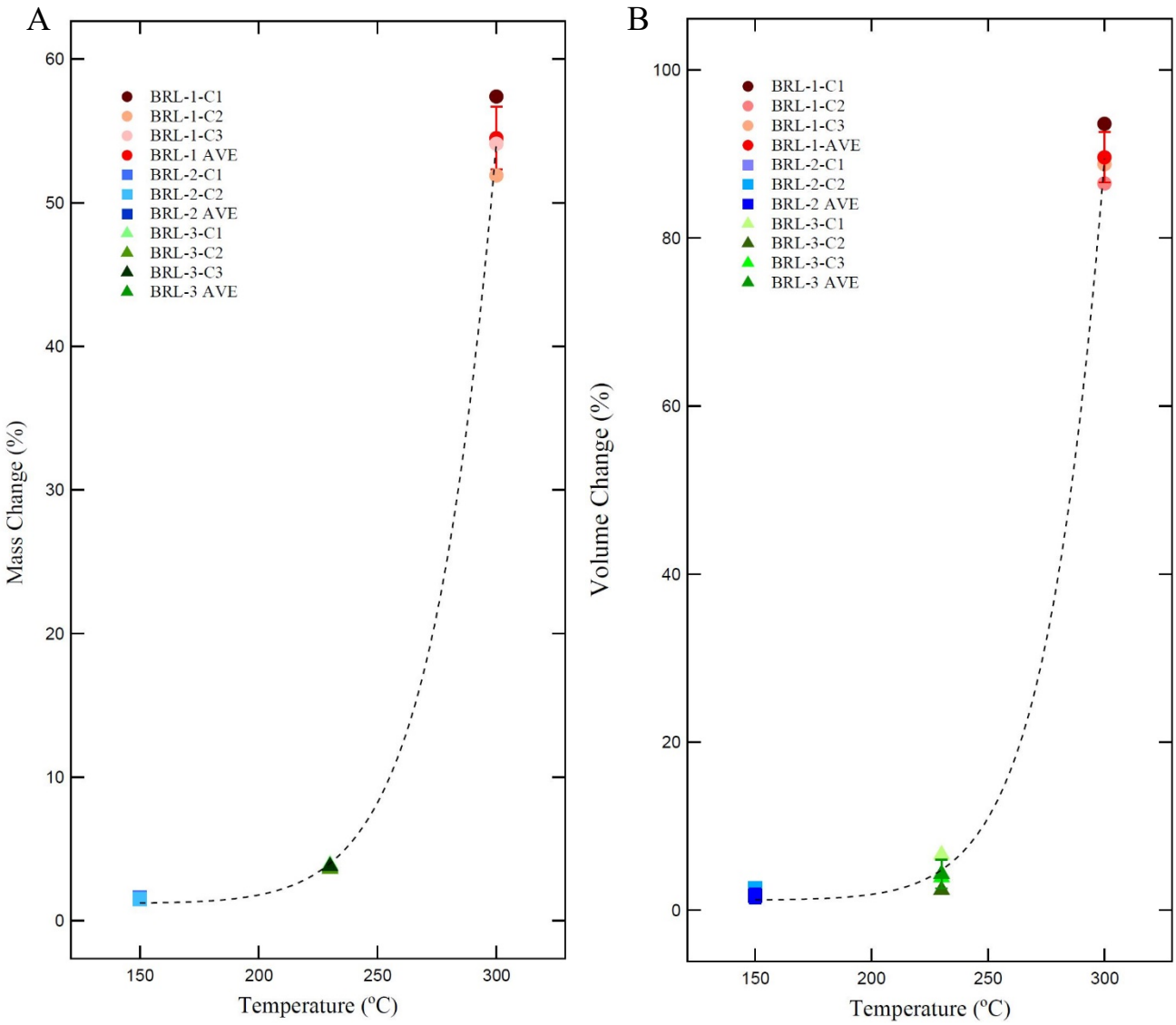

Figure 3: **[A]** The percent mass change of the coupons from each experiment versus the experimental temperature. **[B]** The percent volume change of each experiment versus the experimental temperature.

3.2 Gas Generation

During the course of each experiment, the pressure of the sealed autoclave increased naturally due to gas reaction products from reaction between water and Boral® coupons. Pressure was released from the system to maintain 150 bar when necessary. Gas samples accompanied reaction fluids when sampling through the autoclave exit tube. The gas extracted is likely predominantly H_2 gas based on the components of the experimental system. The volume of the gas extracted (at room temperature) in sampling syringes was estimated and recorded. The

experiments generated the following (minimum) amounts of H_2 gas: BRL-1, 1396.0 mL; BRL-2, 12.6 mL; and BRL-3, 35.7 mL.

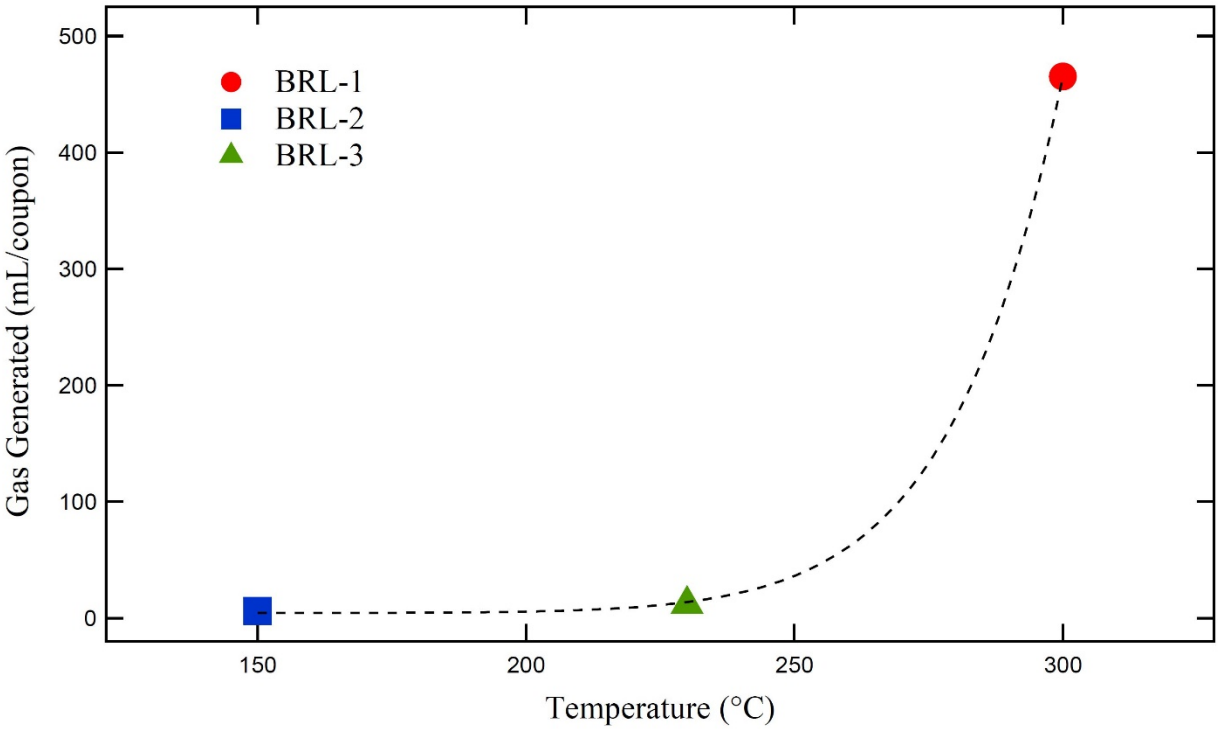

Figure 4: The gas generated from each coupon in the experiments versus the temperature.

3.3 Aqueous Geochemistry

Fluid samples collected weekly and after experiment cooling (quench) showed changes in aqueous chemistry during each experiment. A quench aqueous sample was not collected from BRL-1 due to gold bag rupture during experiment cooling. The main species observed in solution were aluminum and boron (Figure 5). Detailed geochemical modelling has not been performed, but, in general, the 300 °C experiment correspond to the highest concentrations of aluminum and boron. Aluminum concentrations decrease from week one to week two of the 300 °C and 150 °C experiments, but increase in the 230 °C experiment. Boron concentrations are between 15 and 20 mg/L in all experiments, and follow a generally flat trend. The pH at 25 °C of the 300 °C experiment is ~8 in contrast to the lower temperature experiments, which have pH values at room temperature between 6 and 7 (Figure 5). Quench pH values increase in the case of BRL-3 and decrease in BRL-2.

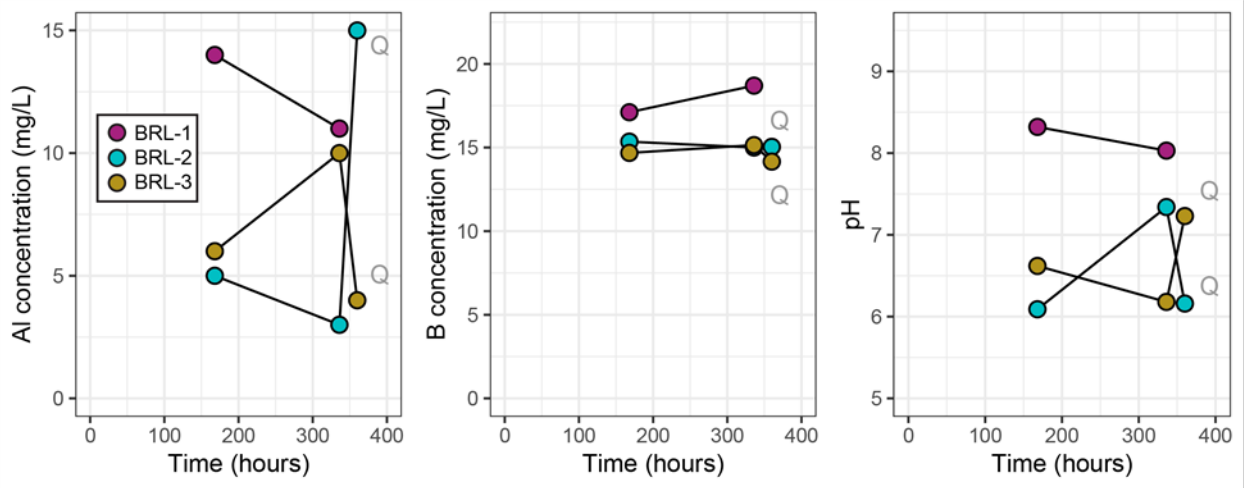

Figure 5: Unfiltered aluminum and boron in solution and pH (at 25°C) plots from BRL-1, BRL-2, and BRL-3. Q–Quench values.

3.4 Mineralogy (X-ray diffraction and scanning electron microscope)

3.4.1 XRD Results

The main alteration product identified by XRD in the reacted Boral® coupons is boehmite (γ-AlO(OH)), a hydrated aluminum oxide mineral. Boehmite formed in the lower temperature experiment (150 °C) is microcrystalline and produces broad X-ray diffraction peaks (Figure 6a). In comparison, boehmite becomes progressively more crystalline at higher temperature, as indicated by sharp, defined XRD peaks (Figure 6a). The alteration of aluminum is pervasive in the 300 °C reaction products and extends throughout the depth of the cladding at the edges of the coupons. Further, alteration of aluminum sinter in the B_4C-Al composite core is observed, but some aluminum is observed to be unaltered. In the core of the 230 °C and 150 °C coupons, alteration to boehmite is minimal. The boron carbide peaks do not show any significant shift, but show slight changes in height and shape with higher temperature.

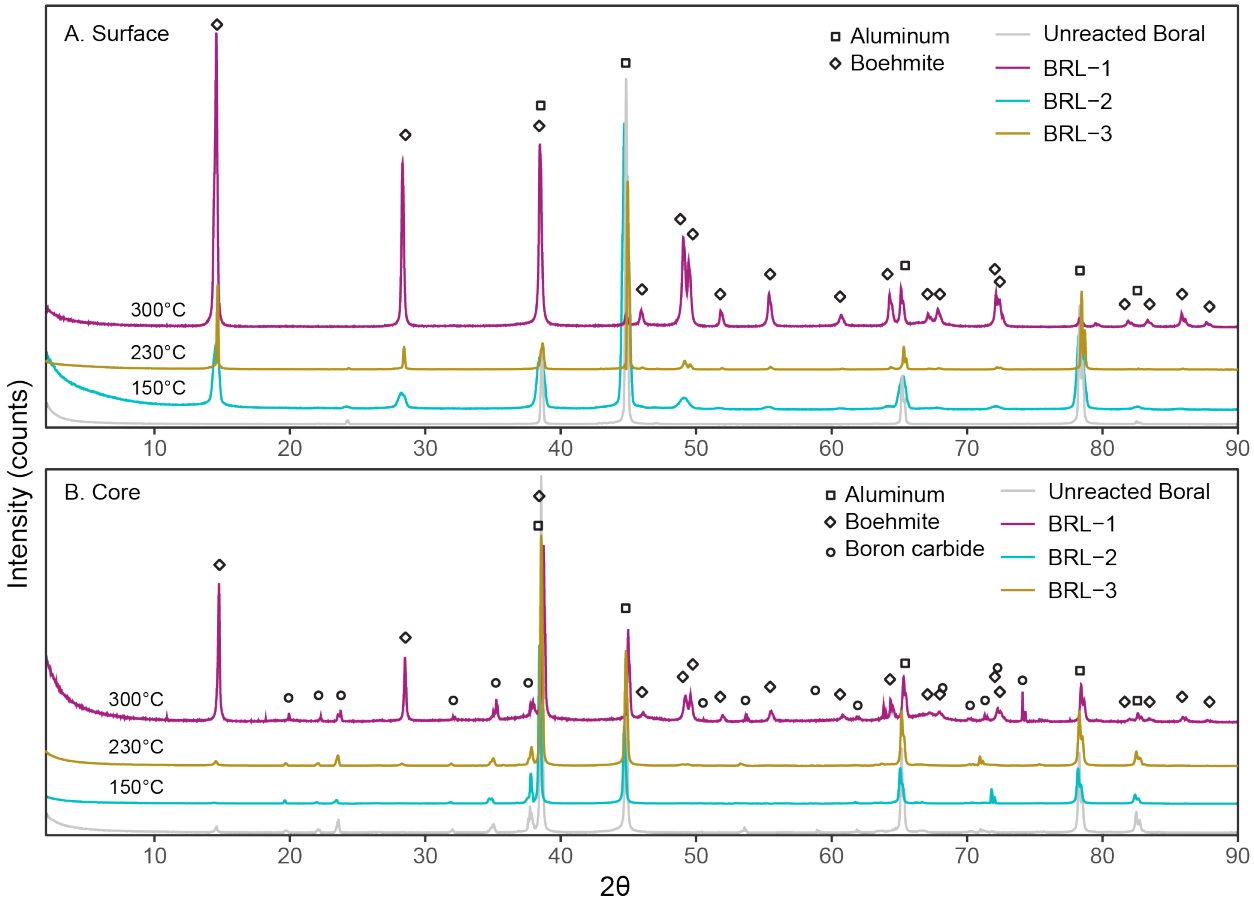

Figure 6: X-ray diffraction patterns for the [A] surface and [B] core of Boral® coupons before and after hydrothermal treatment. Patterns show the alteration of Al cladding and sinter at the coupon surface and interior. Mineral identification was performed with the Jade© 9.5 X-ray data evaluation program with the ICDD PDF-4 database.

3.4.2 SEM/EDS Results

Unreacted and reaction Boral coupons were imaged with scanning electron microscopy. The following describes observations from each set of coupons.

Unreacted coupons: The Al cladding of unreacted Boral coupons displays a rough surface, characterized by parallel, thin striations (Figure 7a). The core is characterized by B_4C crystals (~50 to 250 µm) suspended in a fine-grained Al-sinter matrix.

BRL-1, 300 °C: The SEM images show extensive alteration of the Al cladding to well-formed, crystalline boehmite (Figure 8a). Boehmite crystals are up to ~25 µm in size and have a hexagonal crystal form. Boehmite formation is observed in the coupon composite core at 300 °C,

indicating alteration of Al sinter (Figure 8b). Boehmite crystals in the core are generally finer grained than the crystals formed on the coupon surface.

BRL-2, 150 °C: Boehmite forms a thin, poorly crystalline coating on the surface of the Al cladding in the 150 °C reacted coupons (Figure 8c). Boehmite crystals that are formed on the Al cladding are <<1 µm and do not have a well-defined crystal form. Minor boehmite alteration is observed in the core material at 150 °C.

BRL-3, 230 °C: Boehmite forms a thin coating on the surface of the Al cladding in the 230 °C reacted coupons (Figure 8e). Boehmite displays an elongate, hexagonal crystalline form and are ~1 to 5 µm in diameter. Alteration of Al to fine-grained boehmite is observed in the core material and is more prevalent than at 150 °C. Potential dissolution pits were observed locally on boron carbide grains in BRL-3 reaction products (Figure 8f).

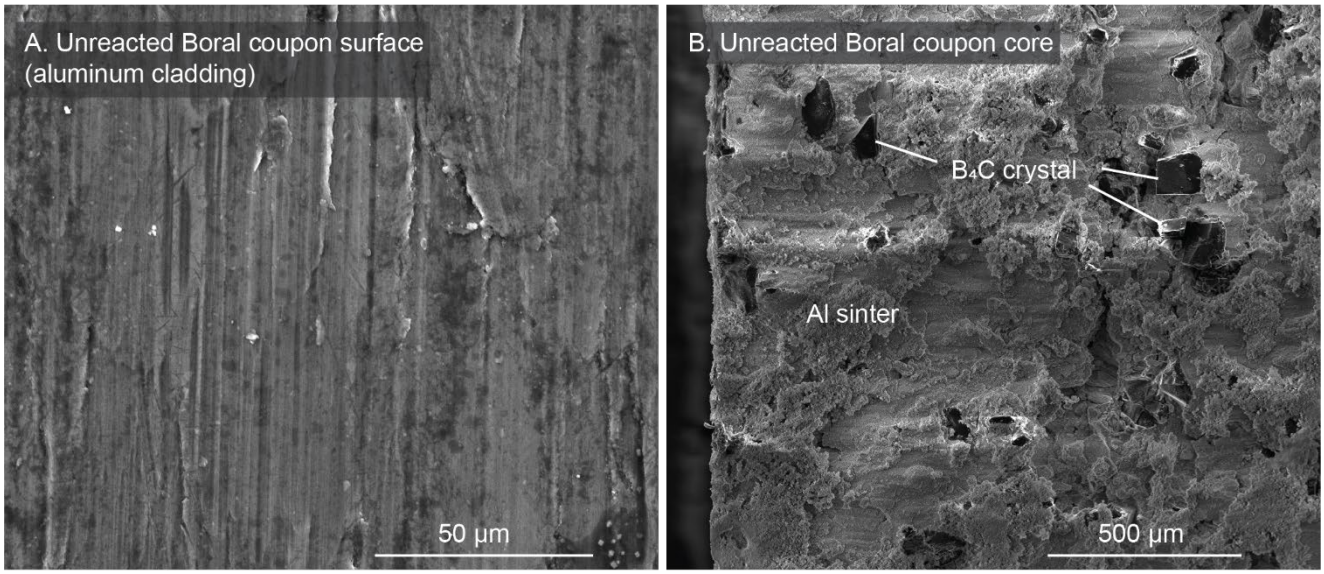

Figure 7: SEM images of unreacted Boral coupons. [A] Coupon surface showing topography of the Al cladding. [B] Composite core of a coupon showing embedded boron carbide crystals in a fine-grained Al sinter matrix.

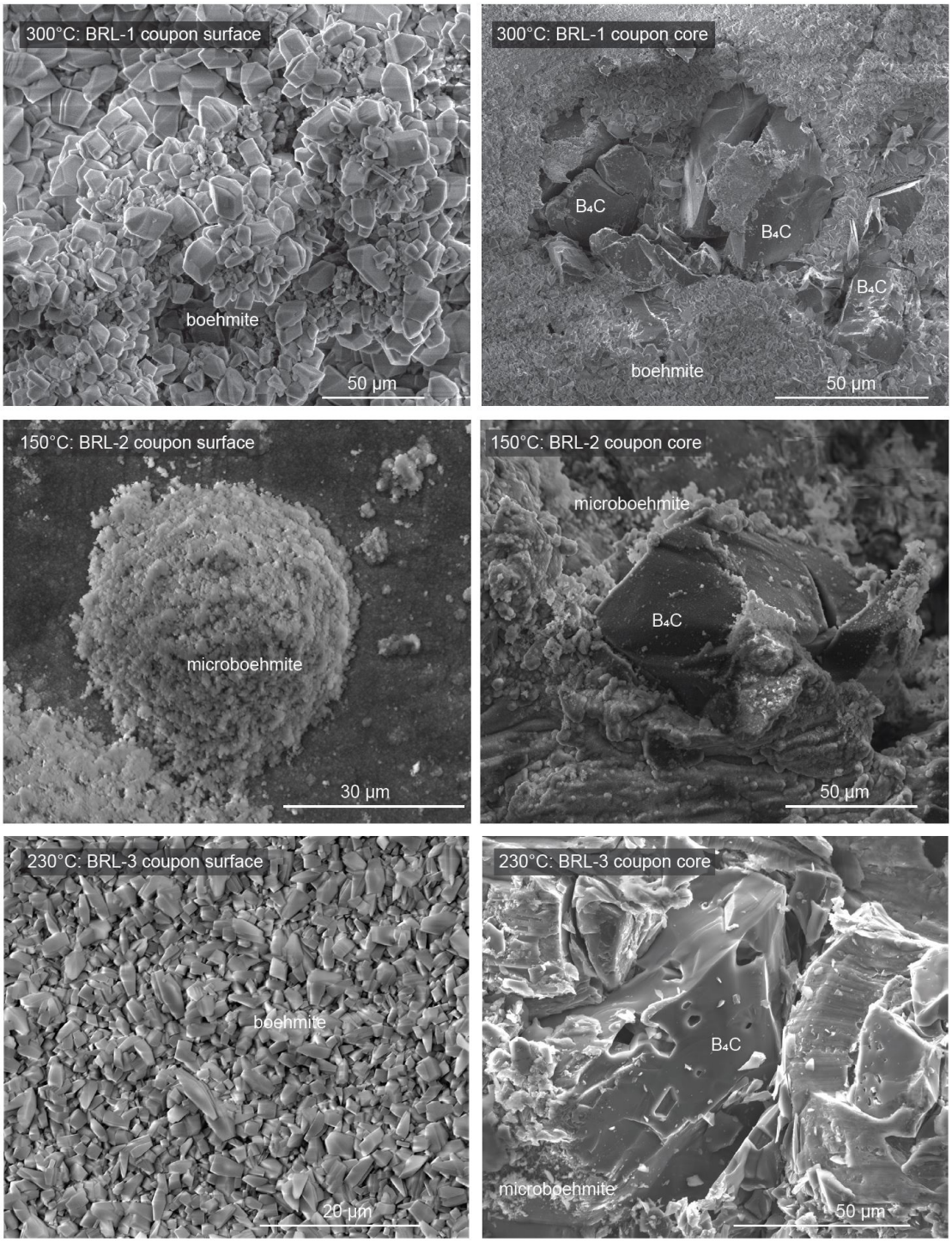

Figure 8: SEM images of post reaction coupons from all experiments. **[A]** Well-formed, hexagonal boehmite crystals on the surface of a BRL-1 coupon. **[B]** Boron carbide crystals embedded in a matrix of fine-grained boehmite (alteration of Al sinter). **[C]** "Microboehmite," or poorly crystalline, fine-grained boehmite on the surface of a BRL-2 coupon. **[D]** Boron carbide crystal in a matrix of Al sinter partially reacted to boehmite. **[E]** Hexagonal boehmite crystals on the surface of a BRL-3 coupon. Note the smaller crystal size and slightly less defined crystal form in comparison to **[A]**. **[F]** Boron carbide grain from experiment BRL-3 in a fine grained boehmite and Al sinter matrix with possible dissolution pitting textures.

4. DISCUSSION

The main results of hydrothermal treatment of Boral® coupons was the alteration of aluminum and the generation of hydrogen gas (H_2). The alteration of Al to boehmite results in physical changes to the Boral® coupons, for example, in the 300 °C experiment, dramatic dimension increases (90% volume increase) and H_2 gas generation (at least 1700 mL). Coupon mass and volume increases and hydrogen gas generation increased exponentially with temperature (Figures 3 and 4). The following reaction describes connected Al alteration and gas generation:

$$2Al_{(s)} + 4H_2O \rightarrow 2AlO(OH)_{(s)} + 3H_{2(g)}$$

Al metal + water → boehmite + hydrogen gas

The mechanism for Al alteration based on our experimental products differs from previous studies that characterize the aluminum corrosion product as Al_2O_3 through the reaction (SAND, 2017):

$$2\ Al_{(s)} + 3H_2O \rightarrow Al_2O_{3(s)} + 3H_{2(g)}$$

Al metal + water → Alumina oxide (corundum) + hydrogen gas

Both reactions above would generate 1.5 mol H_2 gas per 1 mol of aluminum. However, the formation of boehmite involves 2 mol of H_2O per mol of Al in comparison to 1.5 mol of H_2O per mol Al in the formation of corundum. Thus, some hydrogen would be sequestered in during boehmite formation, resulting in less $H_{2(g)}$ generation for a given volume of H_2O. The generation of H_2 gas is a concern for the function of DPC in a disposal scenario (SAND, 2017) and, therefore, the formation of boehmite instead of corundum is important in calculating the amount of H_2 gas liberated in Boral hydrothermal reactions, if H_2O is a limiting reactant.

The aluminum alteration is likely the mechanism for coupon expansion. The mineral boehmite has a unit cell volume of 129 $Å^3$ in comparison to aluminum metal, which has a unit cell volume of 66 $Å^3$. Therefore, the reaction of Al metal to boehmite described above would result in ~97% increase in volume. In the 300 °C experiment, a ~90% increase in volume of the Boral® coupon was observed, likely due to the expansion associated with boehmite formation. The center of the BRL-1 (300 °C) coupon was observed to be less thick than the edges (Figure

2a) and unaltered aluminum is present in the coupon core, indicating that alteration of aluminum was more prevalent at the more porous edges where the composite was directly exposed to water.

Potential alteration of boron carbide (B_4C) is less apparent in SEM images and XRD results. The XRD peaks in higher temperature experiments are less sharp (Figure 6), and potentially indicate degradation of the crystal structure. In addition, increased boron concentration are detected in the reaction fluids (Figure 5). The alteration of boron carbide under hydrothermal conditions may be significant to the function of this material as a neutron absorber. Further, B_4C crystals show dissolution textures in the SEM images from the 230 °C (BRL-3) and 300 °C (BRL-1) experiments (e.g., Figure 8F).

The alteration of the Boral® coupon causes significant changes to the material properties that may affect performance in a repository setting. For example, coupons reacted at 300 °C are brittle and easily snapped with manual force. The expansion of the coupon included swelling, or expansion of the B_4C-Al composite core. This expansion, likely due to the alteration of Al to boehmite results in enlargement of pore spaces and weakening of the composite sinter.

The effects of hydrothermal treatment on boron carbide should be a future topic of study. The preliminary results presented here show some change to the shape of the boron carbide X-ray diffraction peaks at 230 and 300 °C, dissolution textures, and increases in boron in the reaction fluids, indicating some dissolution or mineralogical change could have occurred.

5. CONCLUSION

5.1 Concept Developed

- Boehmite is the alteration product of the aluminum cladding and aluminum sinter in 150, 230, 300 °C hydrothermal experiments with DI water.
- The alteration of aluminum to boehmite is accompanied by increase in Boral® coupon dimensions and masses.
- Hydrogen gas generated.
- Coupon alteration and hydrogen gas generation increases exponentially with temperature.
- Dramatic alteration of Boral® coupons occurred at 300 °C and 150 bar over the course of two weeks.
- Some evidence for B_4C dissolution is observed (e.g., pitting and B in reaction fluids).

5.2 Future R&D

- Detailed examination of B_4C crystallographic changes and potential dissolution.
- Aqueous geochemical modelling of reaction fluids with respect to boehmite and B_4C stability.
- Create a detailed temperature profile of Al alteration.
- Conduct experiments on the effect of the presence of other canister materials, such as stainless steel, on Boral alteration.

6. ACKNOWLEDGEMENTS

We would like to thank George Perkins, Oana Marina and Rose Harris for water chemistry analyses. Scanning electron microscopy facilities were provided by Materials Science and Technology group at Los Alamos National Laboratory. Funding was through the Department of Energy's Spent Fuel and Waste Science and Technology.

7. REFERENCES

Diggle, J.,W., Downie, T.C., and Goulding, C.W. (1969) Anodic oxide films on aluminium. Chem Reviews, ACS publications, pp. 365-405.

EPRI (Electric Power Research Institute) 2009. Handbook of Neutron Absorber Materials for Spent Nuclear Fuel Transportation and Storage Applications: 2009 Edition. 1019110. Palo Alto, CA.

Greene, S.R., J.S. Medford and S.A. Macy (2013). Storage and Transport Cask Data for Used Commercial Nuclear Fuel – 2013 U.S. Edition. ATI-TR-13047. Energy, Oak Ridge, TN, and Advanced Technology Insights, LLC, Knoxville, TN

Greenburg, H.R. and Wen, J. (2013) Repository layout and host rock thermal gradient trade study for large waste packages in clay/shale: Using the DSEF thermal analytical model. LLNL-TR-639869-DRAFT, pp. 38.

Hunter, M.S., and Fowle, P. (1956) Natural and thermally formed Oxide Films on Aluminum. Journal of Electrochemical Society, 103, pp. 482-485.

International Atomic Energy Agency (IAEA) (2000) Multi-purpose container technologies for spent fuel management. IAEA Technical Document, IAEA-TECDOC-1192, pp. 56.

Konings, Dr. Rudy J. M., Allen, Todd R., Stoller, Roger E, and Yamanaka, Prof. Shinsuke. Comprehensive Nuclear Materials. United States: N. p., 2012. Web.

SAND (2017) Joint Workplan for Filler Investigations for DPCs. Sandia National Laboratory, Albuquerque NM. SFWD-SFWST-2018-000481 Rev. 0

Santos, P.S., Coelho, A.C., Santos, H.,, and Kiyohara, P.K. (2009) Hydrothermal synthesis of Well-Crystallized Boehmite Crystals of Various Shapes. Materials Research V 12, # 4, 437-445

Seyfried, J.R., Janecky, D.R., and Berndt, M.E. (1987) Rocking autoclaves for hydrothermal experiments II. The flexible reaction-cell system. Hydrothermal Experimental Techniques. Eds. Ulmer, G.C. and Barnes, H.L. John Wiley & Sons, pp. 216 – 239.

Walters, W.S. (1985) Experimental investigation of corrosion rates and mechanisms in BORAL. Brit. Corr. Jour. V2,#2, pp 84-89

Weeks, J.R. (1978) Corrosion Considerations in the use of BORAL in spent Fuel Storage Pool Racks. Brookhaven National Laboratory Report, BNL-NUREG-25582, 24 p

Wierschke, J.B., (2015) Evaluation of Aluminum-Boron Carbide Neutron Absorbing Materials for interim Storage of Used Nuclear Fuel. Ph.D dissertation, nuclear engineering, University of Michigan.

APPENDIX

Appendix A

Water Chemistry BRL-1 to 3

Appendix B.1. Cation concentrations (ppm)

Sample ID	Filter type	Time (hours)	pH	Cations														
				Al	B	Ba	Ca	Cr	Fe	K	Li	Mg	Mn	Na	Si	SiO_2	Sr	Ti	Zn
BRL-1-1 F Cat	F	168	8.3	1.45	16.90	0.28	0.60	<0.01	0.06	<1.12	0.03	<0.02	<0.01	5.02	17.27	36.97	0.01	<0.01	<0.10
BRL-1-2 F Cat	F	336	8	1.99	18.75	<0.02	0.17	<0.01	0.07	<1.12	0.03	<0.02	<0.01	5.70	12.80	27.38	0.00	0.01	<0.10
BRL-1-1 UF Cat	UF	168	8.3	2.22	17.11	0.04	0.62	<0.01	<0.04	<1.12	0.04	<0.02	<0.01	4.97	19.55	41.83	0.01	0.00	<0.10
BRL-1-2 UF Cat	UF	336	8	1.17	18.70	0.11	0.52	<0.01	0.16	<1.12	0.04	<0.02	<0.01	5.58	11.93	25.52	0.01	0.04	0.20
BRL-2-1 F CAT	F	168	6.1	<0.03	14.96	0.07	0.49	0.01	0.10	3.46	0.02	0.46	<0.01	4.60	1.53	3.27	0.00	<0.01	<0.10
BRL-2-2 F CAT	F	336	7.3	0.04	15.29	0.67	1.21	0.01	0.18	1.42	<0.01	0.47	0.01	<2.50	2.15	4.61	0.02	<0.01	<0.10
BRL-2-3 F CAT	F	360	6.2	<0.03	15.15	0.05	0.30	0.01	0.10	<1.12	<0.01	0.67	0.01	<2.50	0.80	1.71	0.00	<0.01	<0.10
BRL-2-1 UF CAT	UF	168	6.1	0.08	15.35	0.09	0.55	0.01	0.11	2.10	0.02	0.51	0.01	3.31	1.71	3.65	0.00	<0.01	<0.10
BRL-2-2 UF CAT	UF	336	7.3	0.04	15.00	0.10	0.60	0.01	0.09	1.29	<0.01	0.50	0.01	<2.50	1.59	3.41	0.01	<0.01	<0.10
BRL-2-3 UF CAT	UF	360	6.2	2.56	15.04	0.04	0.31	<0.01	0.10	<1.12	<0.01	0.71	<0.01	<2.50	0.67	1.43	0.00	<0.01	<0.10
BRL-3-1 F	F	168	6.6	0.39	14.26	<0.02	0.40	<0.01	<0.04	<1.12	<0.01	0.03	<0.01	<2.50	<0.56	<1.19	0.00	<0.01	<0.10
BRL-3-2 F	F	336	6.2	0.36	14.23	<0.02	0.47	<0.01	<0.04	<1.12	0.01	0.06	<0.01	<2.50	<0.56	<1.19	0.00	<0.01	<0.10
BRL-3-3 F	F	360	7.2	0.44	13.74	<0.02	0.44	<0.01	<0.04	<1.12	0.01	0.08	<0.01	<2.50	<0.56	<1.19	0.00	<0.01	<0.10
BRL-3-1 UF	UF	168	6.6	0.23	14.68	<0.02	0.54	<0.01	<0.04	<1.12	<0.01	0.07	<0.01	<2.50	<0.56	<1.19	0.00	<0.01	0.14
BRL-3-2 UF	UF	336	6.2	0.45	15.14	<0.02	0.66	<0.01	0.04	<1.12	0.02	0.04	<0.01	<2.50	<0.56	<1.19	0.00	<0.01	<0.10
BRL-3-3 UF	UF	360	7.2	0.07	14.16	<0.02	0.35	<0.01	<0.04	<1.12	0.02	0.07	<0.01	<2.50	<0.56	<1.19	0.00	<0.01	<0.10

Appendix B.2. Anion concentrations (ppm)

Sample ID	Filter type	Time (hours)	pH	Anions							
				Bromide	Oxalate	Chloride	Fluoride	Nitrite	Nitrate	Phosphate	Sulfate
BRL-1 (300°C)											
BRL-1-1 UF Cat	UF	168	8.3	<0.1	<0.1	2.56	<0.1	<0.1	<0.1	<0.1	1.75
BRL-1-2 UF Cat	UF	336	8.0	<0.1	<0.1	2.79	<0.1	<0.1	<0.1	<0.1	1.29
BRL-2 (150°C)											
BRL-2-1 UF CAT	UF	168	6.1	<0.1	<0.1	0.42	0.26	<0.1	0.27	<0.1	1.99
BRL-2-2 UF CAT	UF	336	7.3	<0.1	<0.1	9.21	0.32	<0.1	0.21	<0.1	1.05
BRL-2-3 UF CAT	UF	360	6.2	<0.1	<0.1	0.16	0.21	<0.1	0.13	<0.1	1.26
BRL-1 (230°C)											
BRL-3-1 UF	UF	168	6.6	<0.1	<0.1	0.37	<0.1	<0.1	0.108	<0.1	0.63
BRL-3-2 UF	UF	336	6.2	<0.1	<0.1	0.52	<0.1	<0.1	<0.1	<0.1	0.58
BRL-3-3 UF	UF	360	7.2	<0.1	<0.1	0.54	<0.1	<0.1	0.1214	<0.1	0.91

Appendix B

SEM Images

BRL-1

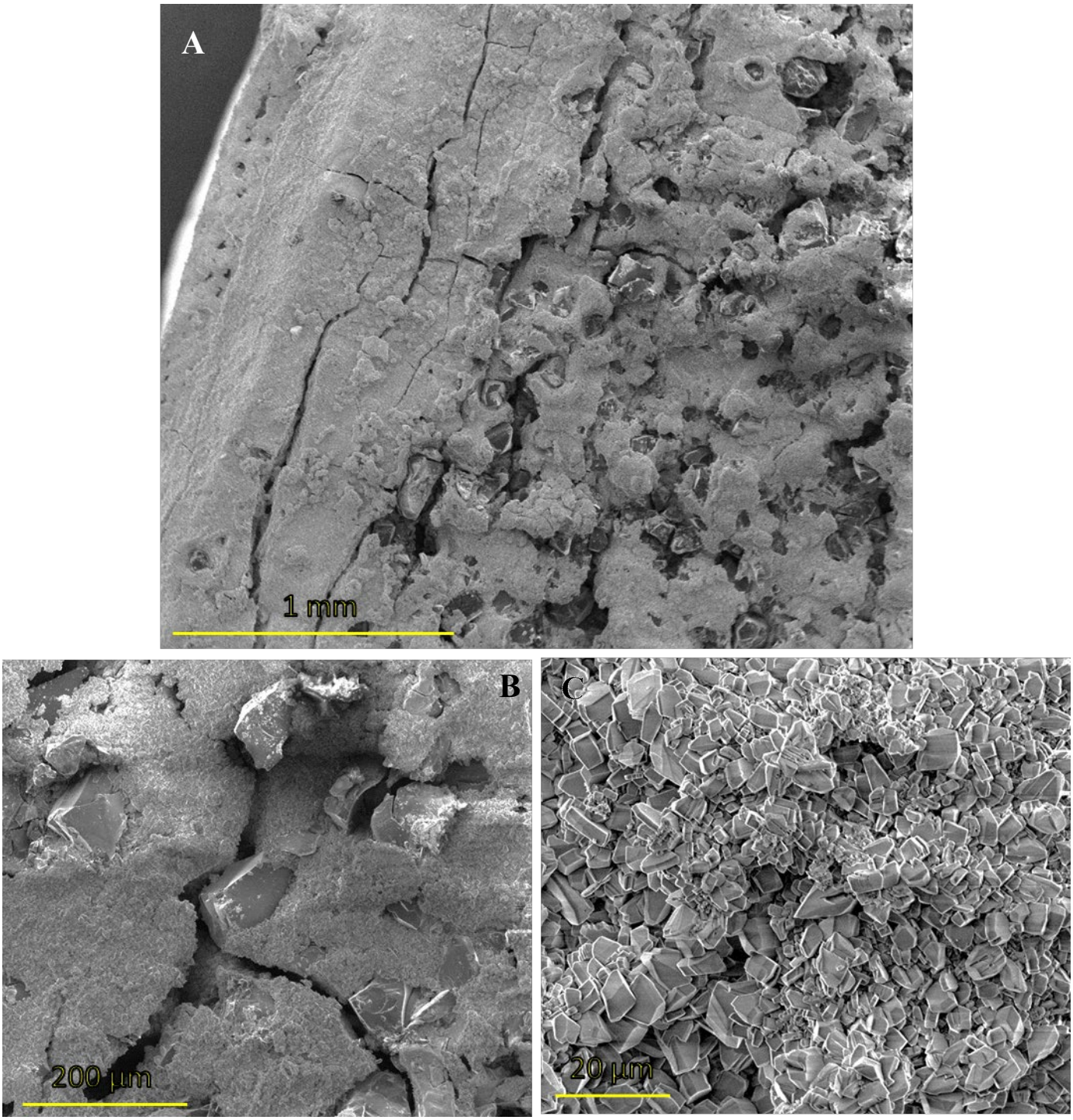

Figure B-1. BRL-1: secondary electron images. **[A]** Exposed B_4C-Al composite on the edge of a coupon. The larger mineral grains are boron carbide surrounded by a fine grained boehmite matrix. **[B]** Boron carbide grains in boehmite matrix. **[C]** Boehmite crystals formed on the Al cladding surface.

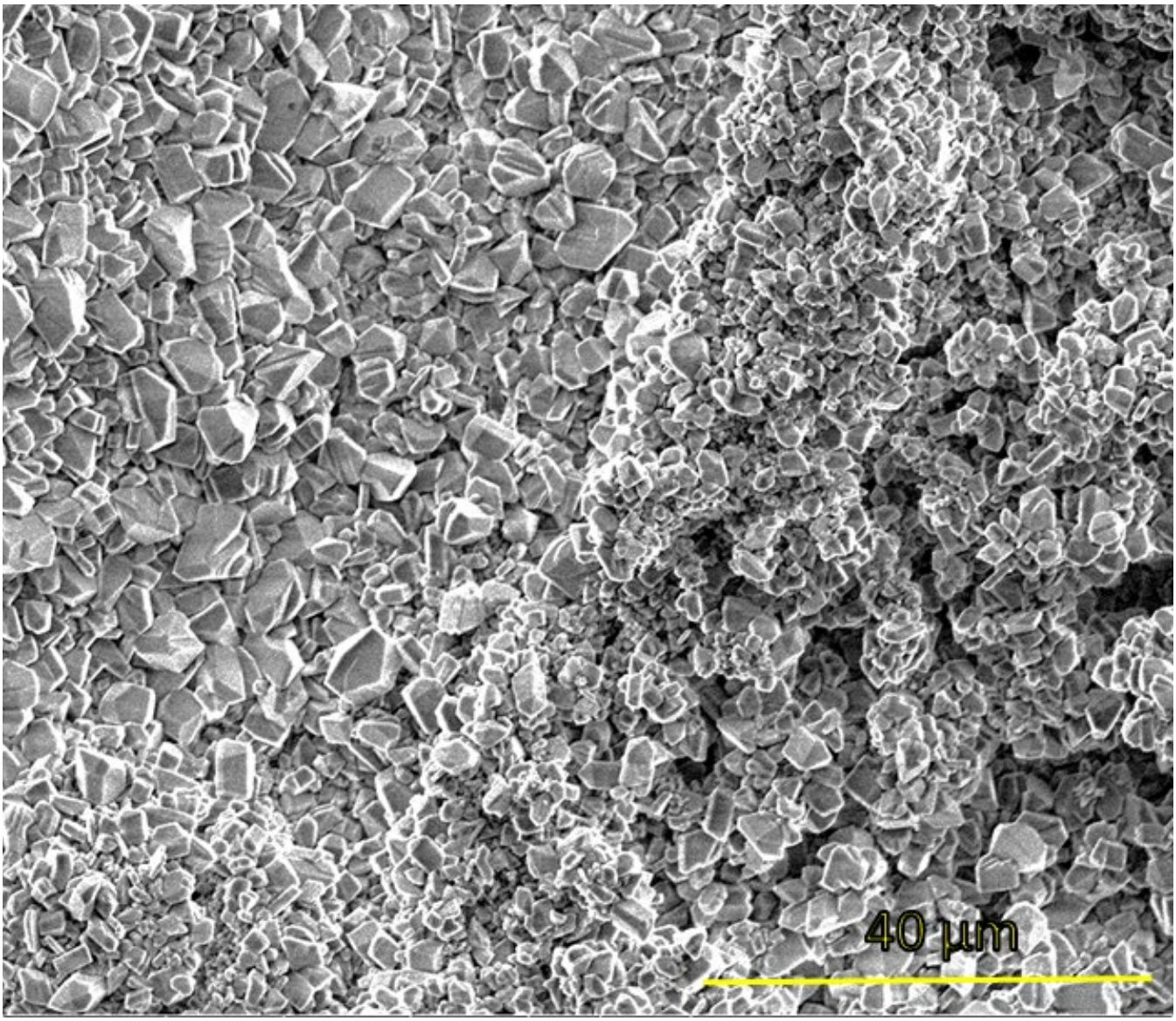

Figure B-2. BRL-1: Hexagonal boehmite crystals on the surface of the reacted Al cladding.

BRL-2

SEM Images

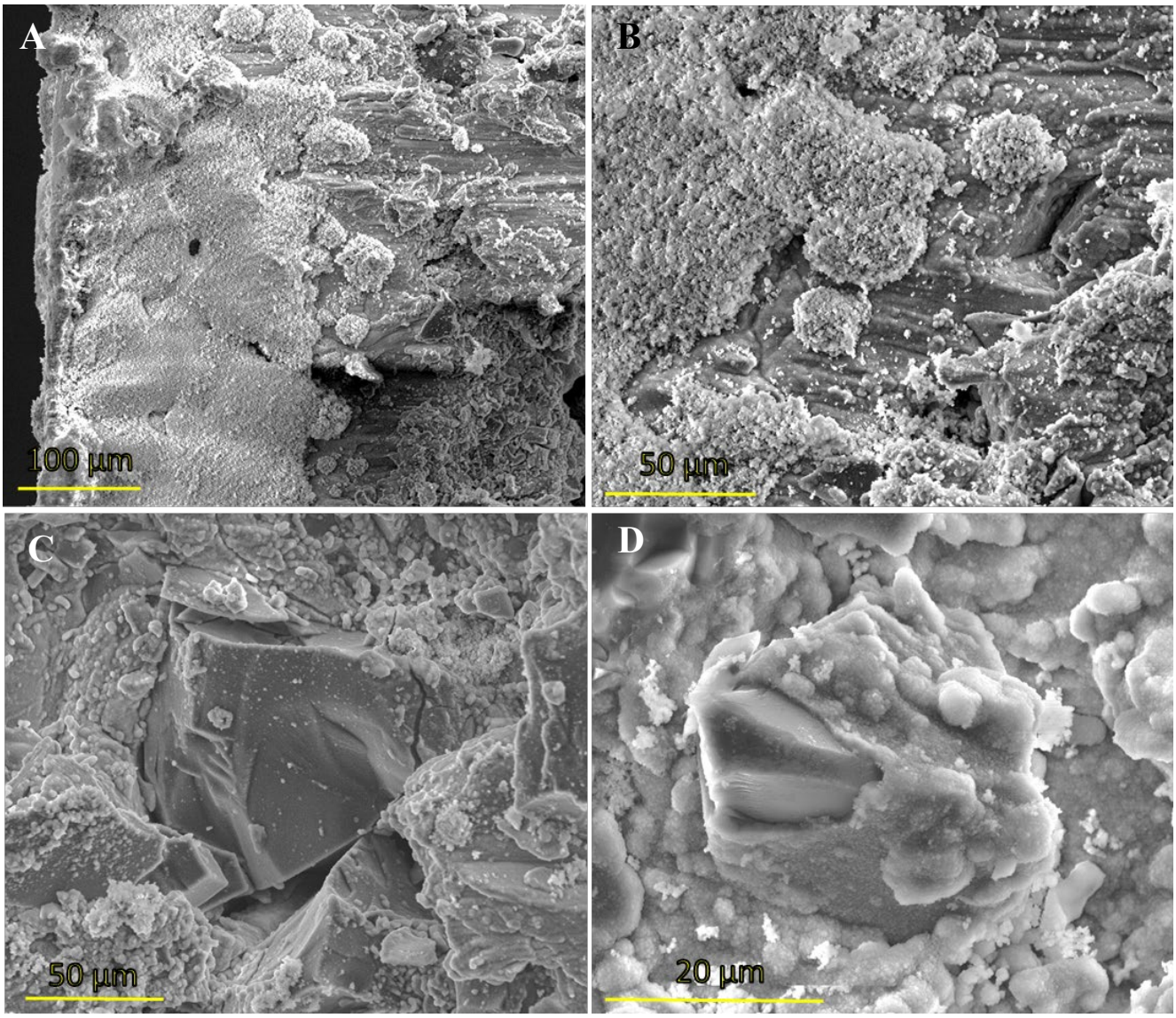

Figure B-3. BRL-2. [A] Exposed, reacted B4C-Al composite on the edge of a coupon that shows alteration of Al sinter to fine grained boehmite. [B] Microcrystalline boehmite on the altered surface of the Al cladding. [C & D] Boron carbide in matrix of fine grained Al sinter that is partially altered to microcrystalline boehmite

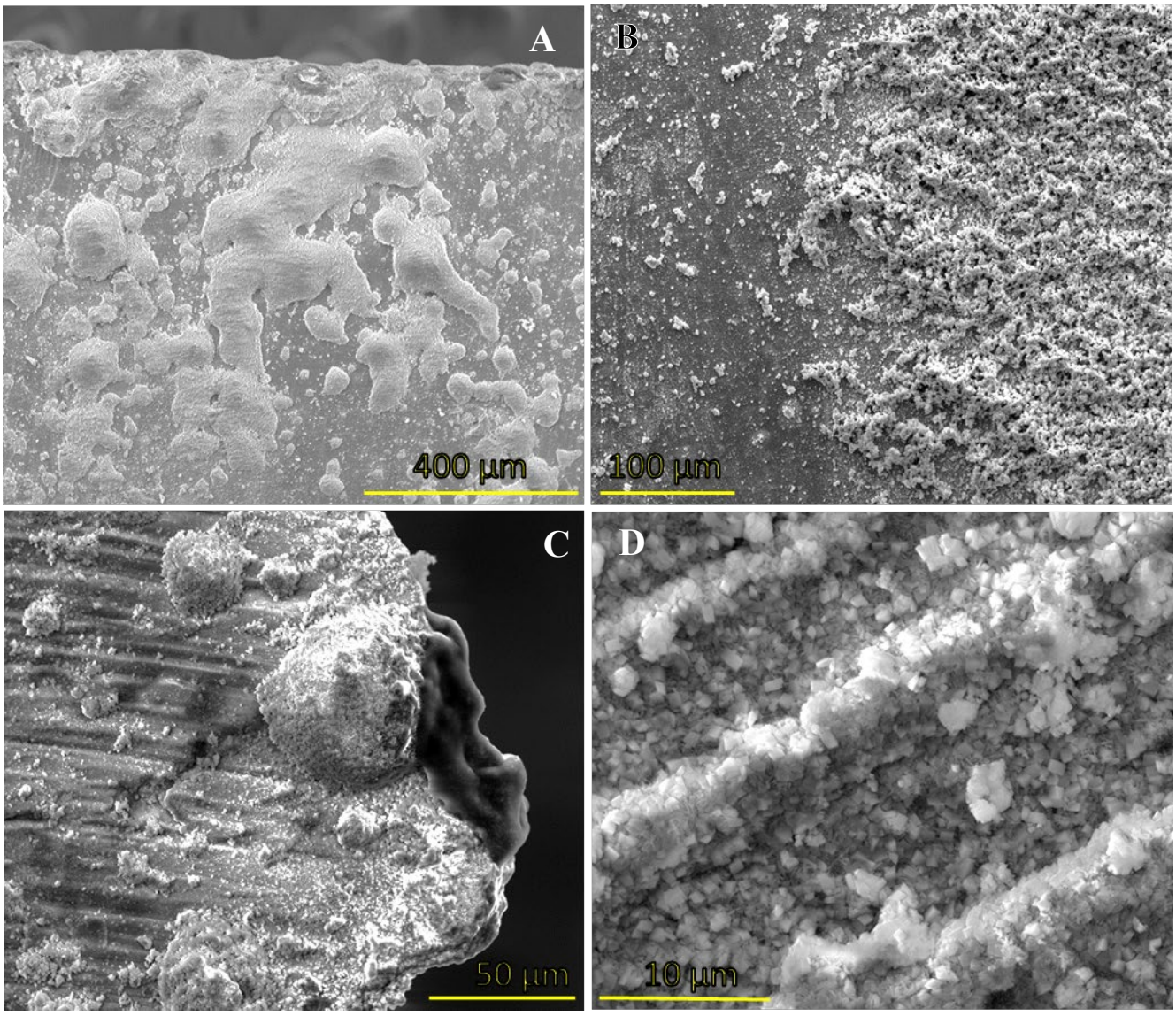

Figure B-4. BRL-2 [A, B, C, & D] Microcrystalline boehmite textures on the altered surface of the Boral coupon. Panels [C & D] show the remnant topography of the striations of Al cladding.

BRL-3

SEM Images

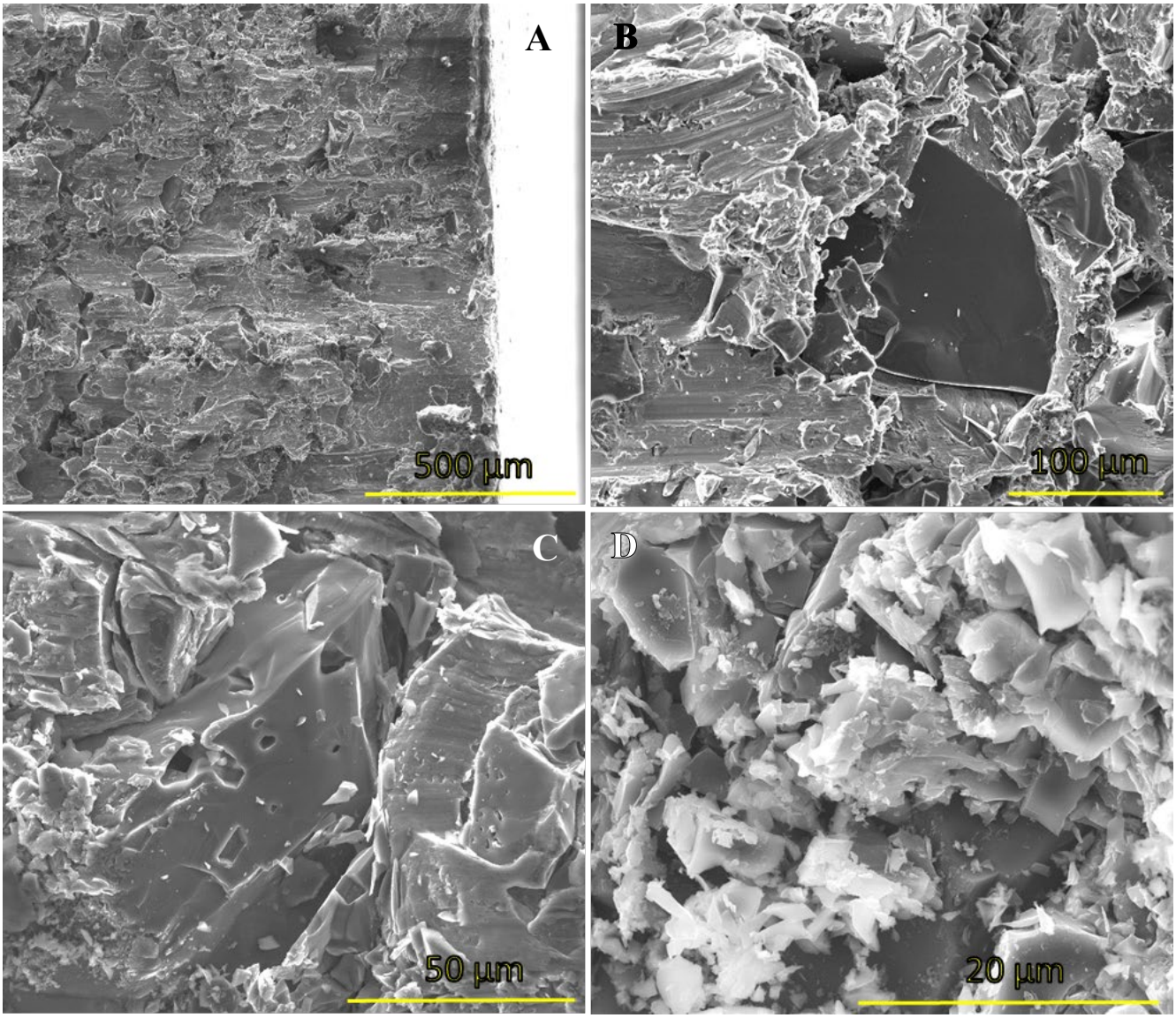

Figure B-5. BRL-3. Alteration on the exposed composed side of a coupon. **[A]** Overview of composite texture. **[B]** Boron carbide grain (center) surrounded by Al sinter and fine-grained boehmite. **[C]** Potential dissolution pitting on a boron carbide grain. **[D]** Light colored boehmite crystals.

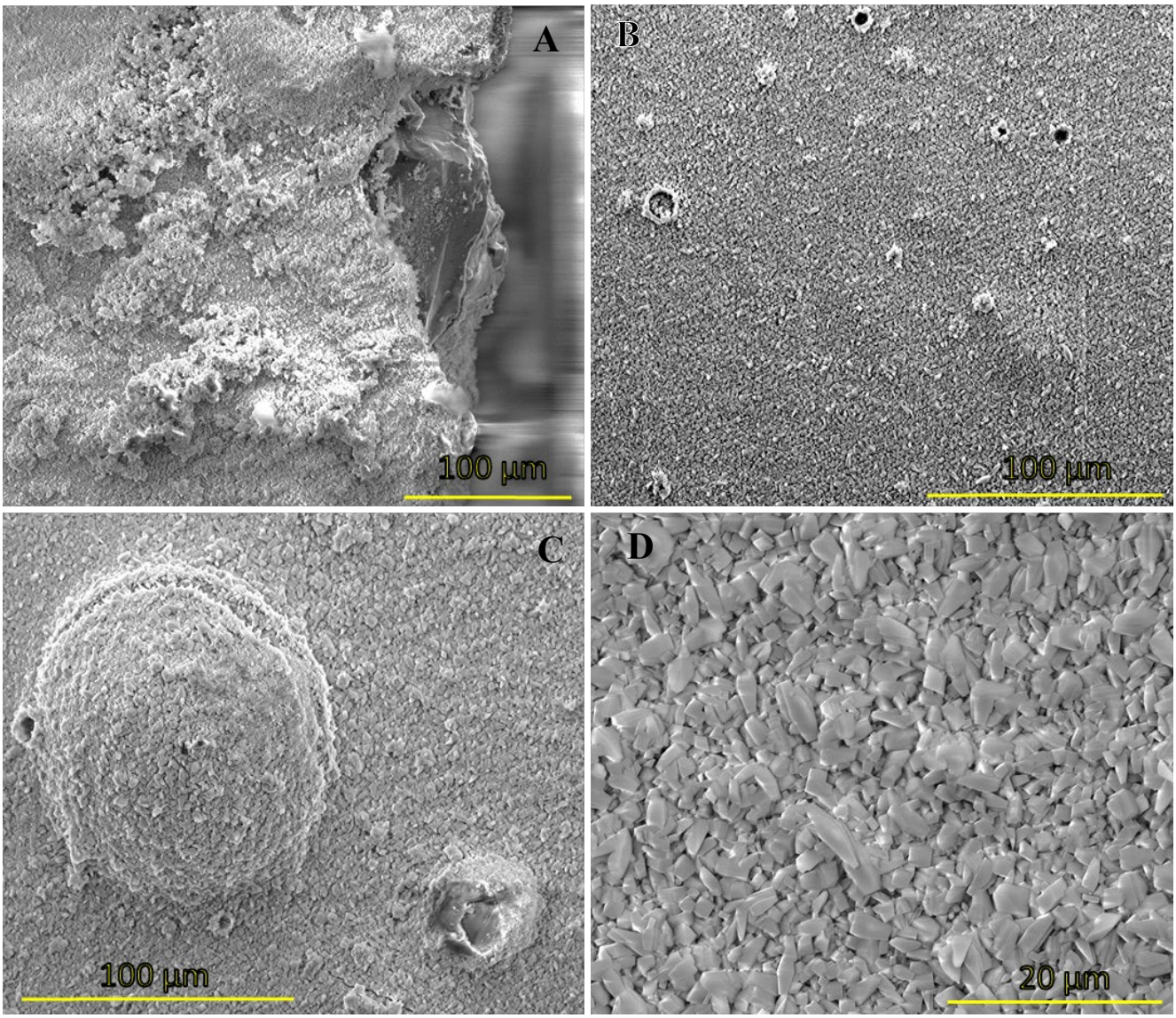

Figure B-6. BRL-3: alteration textures on the surface of the Al cladding. **[A, B]** Overview of boehmite coating on the coupon surface. **[C]** Raised pocket of boehmite on the coupon surface. **[D]** Boehmite crystals are elongate hexagonal and between ~1–5 µm.

Unaltered Boral

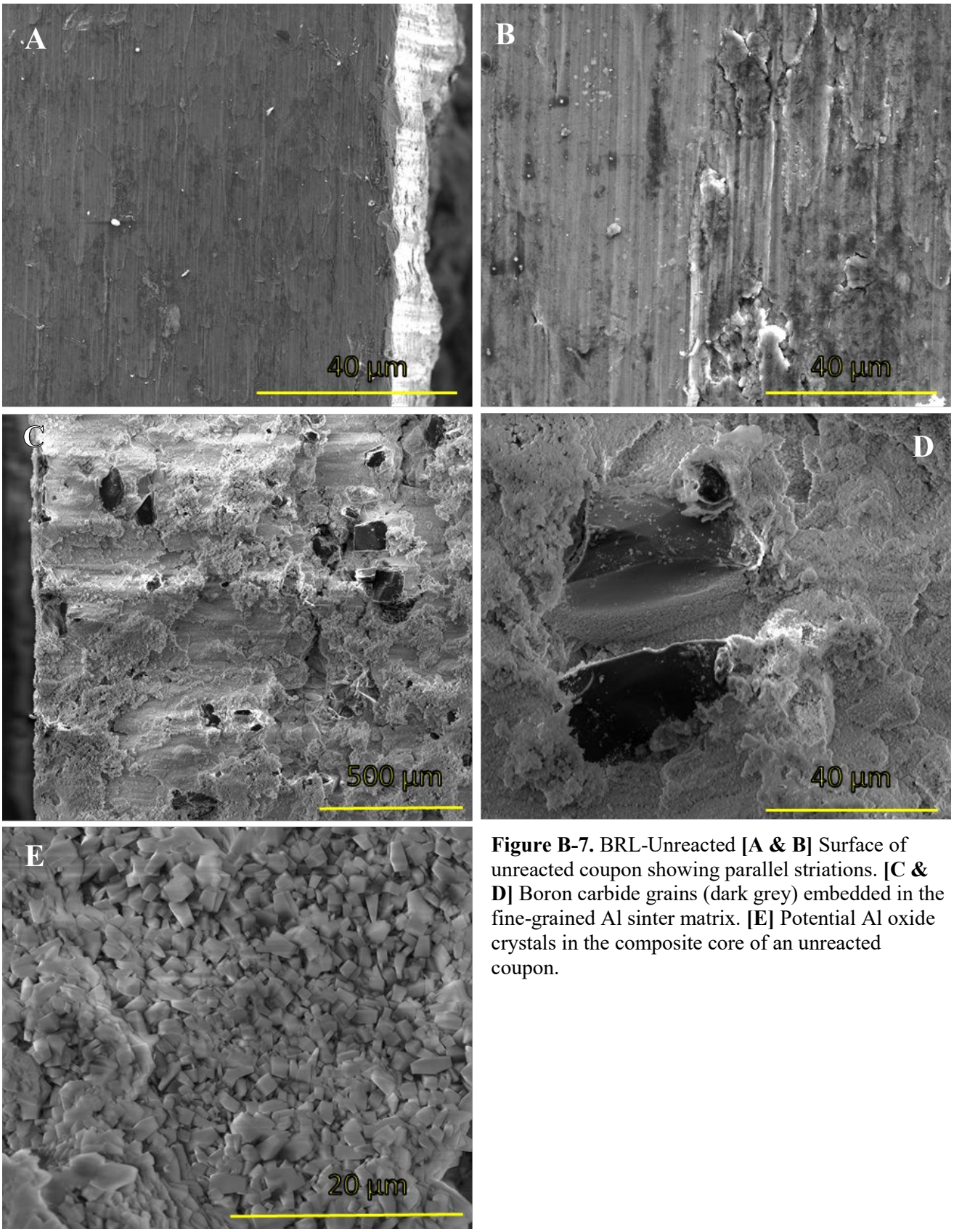

Figure B-7. BRL-Unreacted **[A & B]** Surface of unreacted coupon showing parallel striations. **[C & D]** Boron carbide grains (dark grey) embedded in the fine-grained Al sinter matrix. **[E]** Potential Al oxide crystals in the composite core of an unreacted coupon.

Appendix E

FCT Document Cover Sheet

APPENDIX E

FCT DOCUMENT COVER SHEET [1]

Name/Title of Deliverable/Milestone/Revision No.	Engineered Barrier System R&D and International Collaborations – LANL
Work Package Title and Number	Engineered Barrier System R&D - LANL/ Engineered Barrier System International Collaborations - LANL
Work Package WBS Number	SF-19LA01030801/ SF-19LA01030805
Responsible Work Package Manager	Florie Caporuscio (Name/Signature)

Date Submitted May 10. 2019

Quality Rigor Level for Deliverable/Milestone[2]	☐ QRL-1 Nuclear Data	☐ QRL-2	☐ QRL-3	☒ QRL 4 Lab-specific

This deliverable was prepared in accordance with Los Alamos National Laboratory
(Participant/National Laboratory Name)

QA program which meets the requirements of
☐ DOE Order 414.1 ☒ NQA-1 ☐ Other

This Deliverable was subjected to:

☐ Technical Review ☐ Peer Review

Technical Review (TR)

Review Documentation Provided

☐ Signed TR Report or,
☐ Signed TR Concurrence Sheet or,
☐ Signature of TR Reviewer(s) below

Name and Signature of Reviewers

Peer Review (PR)

Review Documentation Provided

☐ Signed PR Report or,
☐ Signed PR Concurrence Sheet or,
☒ Signature of PR Reviewer(s) below

Name and Signature of Reviewers

Chris Alcorn

REPLACE WITH NEW

NOTE 1: *Appendix E should be filled out and submitted with each deliverable. Or, if the PICS:NE system permits, completely enter all applicable information in the PICS:NE Deliverable Form. The requirement is to ensure that all applicable information is entered either in the PICS:NE system or by using the FCT Document Cover Sheet.*

- *In some cases there may be a milestone where an item is being fabricated, maintenance is being performed on a facility, or a document is being issued through a formal document control process where it specifically calls out a formal review of the document. In these cases, documentation (e.g., inspection report, maintenance request, work planning package documentation or the documented review of the issued document through the document control process) of the completion of the activity, along with the Document Cover Sheet, is sufficient to demonstrate achieving the milestone.*

NOTE 2: *If QRL 1, 2, or 3 is not assigned, then the QRL 4 box must be checked, and the work is understood to be performed using laboratory specific QA requirements. This includes any deliverable developed in conformance with the respective National Laboratory / Participant, DOE or NNSA-approved QA Program.*